Mathematical Models of Fingerprints on the Basis of Lines Description and Delaunay triangulation

Vladimir Gudkov, Chelyabinsk State University, Chelyabinsk, Russia
diana@sonda.ru
Marina Gavrilova, University of Calgary, Canada
marina@cpsc.ucalgary.ca

Abstract. This paper presents a new mathematical model of fingerprints based on representing ridge lines as topological vectors and utilizing Delaunay triangulation for identification. The ridges are stored in the templates with the list of minutiae. Templates are used to identify the fingerprint. This leads to up to 10 times speed-up in processing time while retaining the high degree of identification precision.

Keywords: *Fingerprint, minutiae, topology vector, Delaunay triangulation.*

1. INTRODUCTION

Fingerprint images (FI) identification is realized on the basis of the templates, containing the pattern features. The basis for template identification is minutiae representation in the form of beginnings and endings, junctions and bifurcation of lines [1, 3, 4]. These can be detected by gray image, though in the process of template creation they are guided by the lines skeleton [2, 7, 8] (fig. 1).

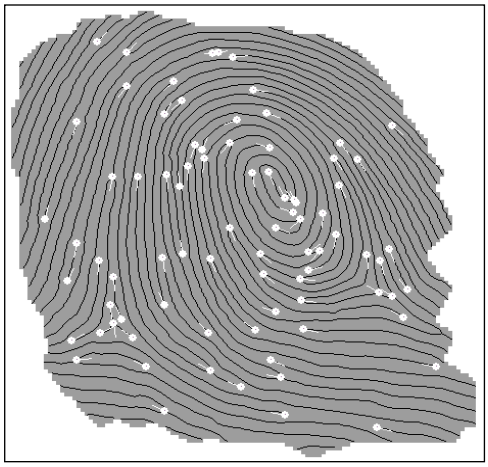

Fig. 1. Skeleton and minutiae points

The mathematical model of the image should depend on necessary and sufficient quantity of features [2]. Minutiae and ridge count between minutiae are reputed as informative in dactyloscopy [7]. However, this count is not present in majority of mathematical models, used in biometrics for automatic proof of pattern uniqueness [8]. Each of such models is focused on increasing the identification accuracy, however suffers from drawbacks of only taking into account limited topological information [5, 6]. For example, classical ridge count, which should be counted along the straight line according to criminalistics, is rarely used due to inherent complexity of processing patterns with curvatures in the area of loops, deltas and whorls [7, 10]. This paper addresses the problem by proposing novel representation and treatment of curved ridge lines through topological vector representation and Delaunay triangulation based methodology.

2. PRELIMINARIES

Voronoi diagram and Delaunay triangulation methods continue to receive compelling attention in the various areas of research, and most recently, in the area of biometrics. From an early article framing computational geometry research as one of powerful vehicles to enhance biometric recognition methods [1, 3], to gamut of current research utilizing geometric properties of biometric data sets [15], the number of attempts to extract geometric information and apply topology to solve biometric problems has increased significantly. There has been research on application of topological methods, including Voronoi diagrams, for variety of biometric recognition systems [3, 6, 17]. In correlation-based matching, two fingerprint images are superimposed and the correlation between corresponding pixels is computed for different alignments [13]. During minutiae-based matching, the set of minutiae are extracted from the two fingerprints and stored as sets of points in the two dimensional plane [3, 4, 15]. While minutiae-matching is most widely used approach in fingerprint recognition, ridge feature-based matching based on orientation map, ridge lines and ridge geometry is frequently overlooked due to complexity of matching algorithm implementation [4].

There have been a number of attempts to utilize Voronoi diagrams in biometric research in other application domains. Voronoi diagrams were used for face partitioning onto segments and facial feature extraction in [17]. A method for binary fingerprint image denoising based on Distance Transform realized through Voronoi method was introduced in [14]. Bebis et. al. [1] used the Delaunay triangle as the comparing index in fingerprint matching. Their method works under assumption that at least one corresponding Delaunay triangle pair can be found between the input and template fingerprint images. As it has been shown in [16], this assumption simply does not hold due to low quality of fingerprint images, distortion in conditions under which fingerprint is obtained, or poor performance of the feature extraction algorithm. Another research supports this position by showing that even small local deformation can cause global deformation up to forty five in edge length [5]. The research presented in this paper takes advantage of additional information, which is ignored by fingerprint matching algorithms – ridge geometry. It is based on ridge line representation as topological vectors and a clever utilization of Delaunay triangulation, which results in increased speed and high recognition capability of the system. The method was fully integrated in a commercial software system and is described by a number of patents [10-12].

3. PROPOSED METHODOLOGY

The templates as a set of FI features are varied in different software systems. Some templates formats are limited in minutiae quantity [7]. Some features of templates are irrelevant, but it is possible to indicate their common property: the templates have features, being some metrics for minutiae points. These metrics are ridge counts between minutiae and topological vector for minutiae [7, 10, 11].

In this paper, an image template is synthesized in the form of

$$\Gamma: F_0^{(m)} \to \{L_m, L_l, L_a\}, \quad (1)$$

where $F_0^{(m)} = \left[f_0^{(m)}(x,y)\right]$ – image skeleton (fig. 1); L_m – minutiae list; L_l – topological vectors list for lines; L_a – accelerator vectors list for lines. Let's introduce some definitions.

Definition 1. The skeleton of the line is simple circuit $\langle u,v\rangle$ with nodes u and v in 8- adjacency, which is near geometrical center of the line, at that there are two adjacent nodes p_2 and p_3 for each node $p_1 \in \langle u,v\rangle$, at that the nodes p_2 and p_3 non-adjacent.

Definition 2. Ending is such node p_1 of the skeleton, that there is one adjacent node p_2 for the node p_1.

Definition 3. Bifurcation is such node p_1 of the skeleton, that there are three adjacent nodes p_2, p_3 and p_4 for the node p_1, at that any two nodes from the multitude $\{p_2, p_3, p_4\}$ are non-adjacent in pairs.

Elements of both topological and accelerator vectors for line are determined using minutiae, which are read from the skeleton nodes as nodes of the graph. These vectors are derivative from the minutiae. However, all these vectors characterize not the area of a separately selected point, but common properties of line as point's multitude or a line segment. In spite of the fact that the lists L_l and L_a characterize FI differently, they are alike in that they represent description for all pattern lines, but not for all points of the lines. This interesting property allows us to synthesize compact templates for very fast matching.

3.1. Minutiae list

We now describe how minutiae list is formed for subsequent fingerprint recognition. Let M_i – is minutiae which is indexed to number i. The minutiae list L_m is in the following form

$$L_m = \{M_i = \{(x_i, y_i), \alpha_i, t_i, v_i, \theta_i, p_i, h_i\} \mid i \in 1..n_1\}, \quad (2)$$

where $|L_m| = n_1$ – cardinal number; (x_i, y_i), α_i, t_i, v_i, θ_i, p_i, h_i – coordinates, direction and type of minutiae, as well as value and direction of curvature, probability and density of lines about minutiae. We propose to detect minutiae detected only in the informative areas. On the fig. 1 FI informative area is darkened, the skeleton is black.

Coordinates (x_i, y_i) of minutiae M_i are determined by coordinates of skeleton node [8, 9]. Direction α_i is determined with circuit of skeleton nodes for line endings and tree circuits for line bifurcations [10]. Type $t_i \in \{0,1\}$ is determined with skeleton nodes valence like the nodes of graph [9], where 0 – bifurcation and 1 – ending. Coordinates (x_i, y_i), direction α_i and type t_i are the basic parameters M_i [7].

Value v_i and direction θ_i of the curvature are determined by lines direction difference in the neighborhood ε of minutiae M_i [10]. Probability p_i is calculated as the ratio of the average value of image quality rating in the neighborhood ε to the best quality rating in the FI informative area [11]. Lines density h_i is calculated as the average quantity of lines, located into the neighborhood ε on the straight line traced transversely to lines [7]. A value of neighborhood ε is assigned to 3-5 line periods.

3.2. Topological vectors list

We now describe how topological vectors are used as effective representation of ridge lines. Topological vectors list for lines L_l is found on the basis of minutia list L_m, skeleton as the matrix $F_0^{(m)}$ and other auxiliary matrixes, elements of which reflect FI local features. These matrixes are formed in the pyramid and shown in fig. 2, which present data informational layers, distributed among its hierarchical structure [2, 7].

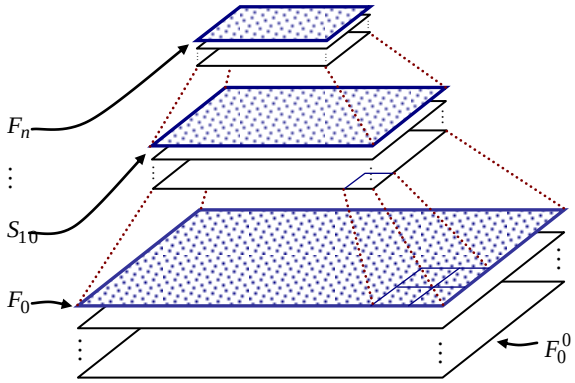

Fig. 2. Hierarchical structure of layers in pyramid

Topological vectors list for lines is synthesized on the basis of all the nodes of skeleton, excluding minutiae nodes, and written in the form of

$$L_l = \{V_i = \{(e_j, n_j, l_j)\} \mid i \in 1..n_2, j \in 1..m_t\}, \quad (3)$$

where V_i – topological vector for skeleton nodes cluster; $|L_l| = n_2$ – cardinal number and $n_2 > n_1$; i – index like the number of topological vector; j – number of link in topological vector; e_j – event, and l_j – length of link, formed with minutiae with number n_j; m_t – quantity of links taking into account central line in the form of

$$m_t = 4m + 2. \quad (4)$$

Let's dwell on the procedure of list synthesis. In the FI informative area the lines are marked out and an image formalized as skeleton is formed. Two types of minutiae are detected on skeleton: endings and bifurcations (fig. 1). Minutiae directions (angle) point to the area of lines number increase [10]. It is parallel to the tangent to papillary line in the small neighborhood of minutiae M_i. Every minutia is numbered and described with coordinates, direction, type, value and direction of curvature, probability and density (2).

Further from each minutia, we draw projections to the right and to the left transversely to the direction vector of the minutiae onto adjacent lines and fix the projections. On the fig. 3, the projections are shown with dotted lines, and two corresponding nodes of skeleton on the lines 1 and 2 are painted over.

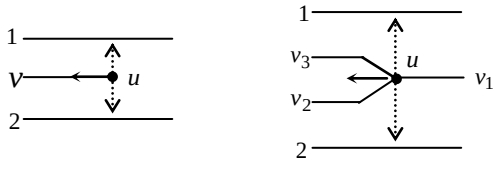

Fig. 3. Projections for ending and bifurcation

Let's choose the skeleton node p_i (not the minutiae) and pass across its coordinates (x_i, y_i) the section to the right and to the

left at a distance of m lines transversely to the tangent to lines being crossed and enumerate on spiral the dissected lines (hereinafter 'links'), which turn clockwise. The section traces the lines curvature [11]. The section depth m is varied from one up to eight lines to the right and the same to the left. One line in the section forms two links. The quantity of links in topological vector is calculated according to formula (4).

Topological vector is determined by the section. To do this, we follow the move of every link by turns on each link, not leaving it and beginning from the section till meeting another minutiae, located on the link, or a projection from minutiae, located on an adjacent line to the right or to the left of the link. The following possible events are detected on the links, shown on the fig. 4 and represented in a binary code.

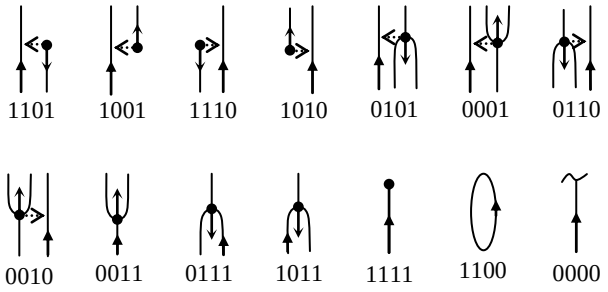

Fig. 4. Events

Minutiae' number initiating the event is associated with the event as the label (fourteen events on fig. 4) detected on the link. The event is associated with the link label. For 0000 and 1100 events the numbers of minutiae are absent. Enumerated set of links with formed events and minutiae' numbers is the ***basic topological vector***. The event and minutiae' number form ordered pair (e_j, n_j). The event is amplified with the link length corresponding to the distance from the section to the position in which the event is detected. ***Enlarged topological vector*** is formed as follows. The event, minutiae' number and length of the link form an ordered triplet (e_j, n_j, l_j). For 0000 and 1100 events the links lengths can describe the informative areas without minutiae. The lengths of links, broken on FI edge, are stable in the meaning that they are not shortened in case of fool rolling of the finger.

Bit location in the event determines minutiae type, its direction regarding the link course, its location regarding the link etc. Events allow on-the-fly compare the ***basic topological vectors*** and speed up the identification procedure.

Topological vectors are built for every node of the skeleton p_i (except minutiae). The process divides the lines into the links, numbered on spiral, turning clockwise. On the fig. 5, examining section for the node A of a skeleton line, which is locked in ending 19, the links are enumerated as 0–17. Topological vector of the node A is shown in the table 1. On the fig. 6, in the section for the node B of the skeleton line, which is locked in bifurcation 19, the links are enumerated as 0–17. Topological vector of the node B is shown in the table 2. The sections are shown with dotted line, and the figures represent usual mutation [11] of ending 19 into bifurcation 19 (which can result due to noise in the original images). Per se the nodes A and B of the skeleton are the same.

The start of links numbering in the section for the nodes A and B (link № 0) is insignificant, as since in case of FI turn over the mirror of links numbers in the section is formed, which is easy recognized and taken into account at FI identification. By analogy with the game «Puzzle» assembling is realized by the way of joining of corresponding connectors. At the section depth $m = 4$ links $m_t = 18$ for the line are formed according to formula (4).

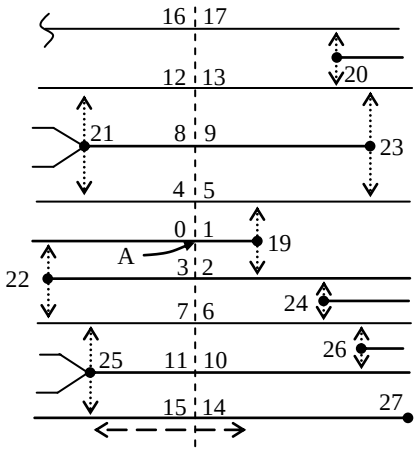

Fig. 5. Section for line with ending

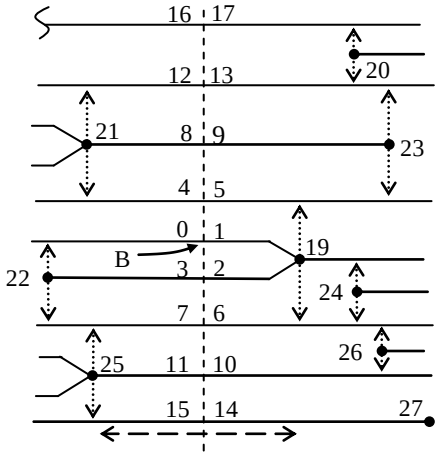

Fig. 6. Section for line with bifurcation

Table 1. Topological vector for A

№	Event	Index	Size
0	1110	22	l_0
1	1111	19	l_1
2	1110	19	l_2
3	1111	22	l_3
4	0001	21	l_4
5	1101	19	l_5
6	1010	24	l_6
7	0010	25	l_7
8	0011	21	l_8
9	1111	23	l_9
10	1010	26	l_{10}
11	0011	25	l_{11}
12	0010	21	l_{12}
13	1010	20	l_{13}
14	1111	27	l_{14}
15	0001	25	l_{15}
16	0000	–	–
17	1001	20	l_{17}

Table 2. Topological vector for B

№	Event	Index	Size
0	1110	22	l_0
1	1011	19	l_1
2	0111	19	l_2
3	1111	22	l_3
4	0001	21	l_4
5	0101	19	l_5
6	0110	19	l_6
7	0010	25	l_7
8	0011	21	l_8
9	1111	23	l_9
10	1010	26	l_{10}
11	0011	25	l_{11}
12	0010	21	l_{12}
13	1010	20	l_{13}
14	1111	27	l_{14}
15	0001	25	l_{15}
16	0000	–	–
17	1001	20	l_{17}

The quantity of topological vectors can be enumerated. At the foot of the fig. 5 with two-forked dotted arrow is shown the zone, located between minutiae 19 and 25, within the bounds of which for the point A at its displacement on the skeleton the same ***basic topological vector*** is synthesized. The similar zone between minutiae 19 and 25 for the point B is shown at the foot of the fig. 6. Topological vectors with equal ***basic topological vectors*** are integrated into one corresponding enlarged topological vector, where the minimum length of link is maximal [11]. At that their quantity is reduced by dozens of times from the value $n_2 < 1000$ to the value $n_1 < 100$ according to (3). Vector V_i automatically characterizes the line or the line segment, but not the minutiae. The image deformation, especially linear, practically does not have any effect upon the content of the basic topological vector. Therefore the vector is named as topological [10-12].

The proposed methodology has series of advantages. Firstly, the section is built along the curved line, which traces curvature direction of the crossed lines. Secondly, at the events calculation the projection of minutiae is used, that result in prevention of the information loss. Thirdly, the links enumerating is turning along the gyrate without links omission. Fourthly, at integration it is possible to choose topological vector with maximum value of minimal length of link [11]. This raises stability and comprehension of mathematical model.

3.3. Delaunay triangulation

After the topological vectors has been defined, we propose to utilize Delaunay triangulation for their matching. Delaunay triangulation is built from the minutia list L_m according to formula (2). By definition, Delaunay triangulation is a triangulation, where circle, circumscribed around any of it's triangle, doesn't contain inside any other point from L_m. For the node A of skeleton line (look the fig. 5) one of triangles is shown on the fig. 7. Vortexes of that triangle are the minutia $\{U_i \,|\, U_i \in L_m, i \in 1..3\}$ and $\{U_i\} = \{M_j \,|\, M_j \in L_m, j \in \{22,21,19\}\}$ accordingly.

To choose the initial vortex of triangle let's note that node A placed inside the circle, circumscribed around the marked triangle. Topological vector for the point A divides an image with its section into two areas. To the area, containing the most quantity of vortexes of marked triangle, direct an ordinate axis of topological vector, and on the section – abscissa axis. Let's choose the initial vortex of triangle U_s with plus ordinate and minimum abscises' meaning. On the fig. 7 minutia number 22 corresponds to vortex U_s.

Let's go clockwise round the vortexes of the triangle, beginning from the vortex U_s. In the sequence of minutia 22, 21, 19 let's compare the lengths of triangle sides $s_1 > s_2, s_2 > s_3, s_3 > s_1$ and form three bits $\gamma_1, \gamma_2, \gamma_3$, where $\gamma \in \{0,1\}$. They are determined with binary results of comparison. It is possible in total 7 states of those bits: 110, 011, 101, 100, 010, 001, 000. The last corresponds to equilateral triangle.

According to the events in topological vector for the point A (table 1) minutiae number 22 is directed contrariwise to the link course. This fact allows us to show the meaning of bit $\gamma_4 = 1$. Therefore, during the clockwise round, over the vertices of triangle sequentially, we calculate $\gamma_5 = 0$ (is directed along the link course) and $\gamma_6 = 1$. Since the minutia distribution is random, there are eight possible states of those three bits.

Node A placed on a line, beginning from minutia 19. If it is directed along ordinate axes of topological vector, let's set the bit $\gamma_7 = 1$, otherwise $\gamma_7 = 0$.

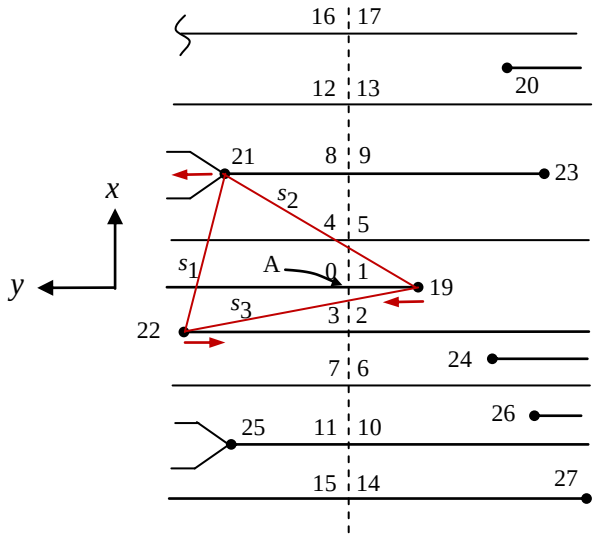

Fig. 7. Delaunay triangulation for A

Calculated bits $C = \{\gamma_k \,|\, k \in 1..7\}$ assume 112 possible states ($7 \times 8 \times 2$). These bits are not correlating. There density of distribution is inhomogeneous. So, we have 112 descriptors which classify topological vectors. Such preliminary classification of topological vectors and minutia on their "equivalence" stable to turns and displacements of the image and speed up fingerprint identification ten times. If n_2 – cardinal number (3), accelerator vectors list is written in the form of

$$L_a = \{ C_i = \{ \gamma_k \,|\, k \in 1..7 \} \,|\, i \in 1..n_2 \}. \quad (5)$$

4. CONCLUSION

In this paper, we presented mathematical model of FI on the basis of topological vectors for the ridge lines, which is stored in the template. Topological vectors form linked graph with a high level of redundancy. This allows connecting sub graphs of fragmentary latents of fingerprints. List L_l according to (3) can be represented in economic format (without links lengths). Minutiae mutation does not change the links enumerating and

minutiae enumeration queue (tables 1, 2), that increases stability of mathematical model.

Topological vectors stability is additionally increased by integrating basic topological vectors into one corresponding enlarged topological vector, where the minimum length of link is maximal.

Additionally, the lines in the areas of loops, deltas, whirls and essential curvatures are automatically divided with topological vectors independently from minutiae location, which increases stability of mathematical model.

Robust descriptions are proposed on the basis of Delaunay triangulation, which form 112 classes and allow speeding up fingerprint identification ten times. We tested fingerprints from optical sensor FVC2000 DB3, FVC2002 DB1, FVC2004 DB1, FVC2006 DB2 on the processor Intel Pentium D CPU 3.40GHz.

An image template according consists of lists which are mutually complementary, for them minutiae list is the determining one. The lists are essentially different and do not replace each other, but one of these lists can be excluded from this template. Moreover, topological vectors can be stored compactly (without links lengths). This allows to further optimize memory capacity for the template storage

5. REFERENCES

[1] Bebis, G., Deaconu, T and Georiopoulous, M. Fingerprint identification using Delaunay triangulation, ICIIS99, Maryland, Nov, pp. 452-459, 1999.

[2] Gonzales, R. Digital processing of the images / R. Gonzales, R. Woods; translation from English; the editor P. Chochia – M.: Techno sphere, 2006. – 1072 p.

[3] Jain, A., Hong, L. and Bolle, R. On-line fingerprint verification, IEEE TPAMI, vol. 4, pp. 302–313, 1997.

[4] Jiang, X., Yau, W.-Y, 2000. Fingerprint minutiae matching based on the local and global structures. In: Proc. 15th Internet. Conf. Pattern Recognition (ICPR, 2000) 2. pp.1042–1045, 2000.

[5] Kovacs-Vajna, Zs. Miklos A Fingerprint Verification System Based on Triangular Matching and Dynamic Time Warping, IEEE Trans. on PAMI, Vol.22, No.11, pp.1266-1276, 2000.

[6] Liang, X. and Asano, T. A Linear Time Algorithm for Binary Fingerprint Image Denoising Using Distance Transform, IEICE TRANSACTIONS on Information and Systems, vol. E89-D, no. 4, pp. 1534-1542, 2006.

[7] Maltoni, D. Handbook of fingerprint recognition / D. Maltoni, D. Maio, A.K. Jain, S. Prabhakar. – London: Springer-Verlag, 2009. – 496 p.

[8] Mestetskiy, L.M. Continious morphology of binary images / L.M. Mestetskiy.– M.: Fizmatlit, 2009.– 288 p.– ISBN 978-5-9221-1050-1.

[9] Novikov, F. Discrete Mathematics for programmers: manual / F. Novikov. – St. Petersburg: Piter, 2001. – 304 p.

[10] Patent 2321057 Russian Federation, Int. Cl. G 06 K 9/52, A 61 B 5/117. The Method of Papillary Pattern Print Coding / V. Gudkov – № 2006142831/09; Field: Dec. 04, 2006; Date of patent: Mar. 27, 2008; Bull. № 9. – 13 p.

[11] Patent 236086 Russian Federation, Int. Cl. G 06 K 9/00, The Method of Papillary Pattern Print Coding / V. Gudkov, A. Bokov, A. Mosunov. – № 2007118575/09; Field: May. 18, 2007; Date of patent: Nov. 27. 2008; Bull. № 33. – 13 p.

[12] Patent 5631971 USA, Int. Cl. G 06 K 9/00. Vector based topological fingerprint matching/ M.K. Sparrow (Winchester). – Field: Jul. 15, 1994; Date of patent: May. 20, 1997; U.S.Cl. 382/125. – 17 p.

[13] Ratha, N.K., Karu, K., Chen, S. and Jain, A. A Real-Time Matching System for Large Fingerprint Databases, PAMI Vol.18, No.8, pp. 799-813, 1996.

[14] H. Wang, M. Gavrilova, Y. Luo and J. Rokne An Efficient Algorithm for Fingerprint Matching, International Conference on Pattern Recognition ICPR 2006, 20 - 24 August 2006, Hong Kong, IEEE-CS publisher, pp. 1034-1037, 2006

[15] Wayman, J, Jain. A, Maltoni, D. and Maio, D. "Biometric Systems: Technology, Design and Performance Evaluation," Book, Springer-Verlag, 2006.

[16] Wang, C. and Gavrilova, M. Delaunay Triangulation Algorithm for Fingerprint Matching IEEE-CS proceedings, ISVD 2006, pp. 208-216, Banff, AB, Canada, July 2006.

[17] Xiao, Y. and Yan, H. Facial Feature Location with Delaunay Triangulation/Voronoi Diagram Calculation, Conferences in Research and Practice in Information Technology, 11. Feng, D. D., Jin, J., Eades, P. and Yan, H., Eds., ACS. 103-108, 2002.

About the author

Vladimir Gudkov, professor at Chelyabinsk State University, Department of Applied Mathematics. His contact e-mail is diana@sonda.ru.

Marina Gavrilova, PHd, University of Calgary, Canada. Her contact e-mail is marina@cpsc.ucalgary.ca.